

*DISTRIBUTION OF DENSITY OF PROTONS WITH GIVEN ANGULAR MOMENTUM IN THE NUCLEUS*

L. P. RAPOPORT and S. G. KADMENSKIĬ

Voronezh State University

Submitted to JETP editor June 2, 1959

J. Exptl. Theoret. Phys. (U.S.S.R.) **37**, 1303-1307 (November, 1959)

The density of protons of given angular momentum is computed from the experimental distribution of the total proton density. Spatial separation of nuclear shells is demonstrated using the distribution thus obtained.

**1. METHOD OF CALCULATION**

THE Thomas-Fermi statistical theory can be generalized so as to give the distribution of density of fermions with angular momentum.<sup>1</sup>

Expanding plane waves in eigenfunctions of the angular momentum, we have

$$\begin{aligned} \rho(r) &= \lim_{r' \rightarrow r} \rho(r, r') = \lim_{r' \rightarrow r} \frac{2}{h^3} \int_0^{P_\mu(r)} \exp(ip(r-r')/h) dp \\ &= \frac{4}{2\pi r} \sum_{l=0}^{\infty} (2l+1) \int_0^{K_\mu(r)} k J_{l+1/2}^2(kr) dk, \quad K_\mu(r) = 2\pi P_\mu(r)/h, \end{aligned} \tag{1}$$

where  $P_\mu(r)$  is the Fermi momentum and  $l$  is the angular momentum quantum number.

From Eq. (1) it can be seen that if one introduces

$$\rho_l(r) = \frac{4}{2\pi r} (2l+1) \int_0^{K_\mu(r)} k J_{l+1/2}^2(kr) dk, \tag{2}$$

such that

$$\rho(r) = \sum_{l=0}^{\infty} \rho_l(r), \tag{3}$$

then the  $\rho_l(r)$  so defined is the density of fermions with given angular momentum  $l$ . From Eqs. (1) and (2) it is clear that knowing

$$K_\mu(r) = [3\pi^2 \rho(r)]^{1/3}, \tag{4}$$

from the distribution of total density  $\rho(r)$ , it is possible to calculate  $\rho_l(r)$  for arbitrary  $l = 0, 1, 2, \dots$ . Equation (2) can be used to calculate the distribution of protons with angular momentum in the nucleus if one takes for the density  $\rho(r)$  the experimental values obtained from the experiments on electron scattering by nuclei.<sup>2</sup>

In this case, since we do not solve the complete dynamical problem of motion of nucleons in the nu-

cleus, the difficult problem of the applicability of the Thomas-Fermi model to the nucleus can be partially avoided. The experimental density automatically takes into account all characteristics of proton motion in the nucleus (type of nuclear force, influence of neutrons, etc.). Considering that the expansion of the plane waves in Eq. (2) is in terms of the exact eigenfunctions of the angular momentum operator, one might expect the application of this formula in our calculation to be more successful than is the case in the usual statistical theory.

We compare, for example, Eq. (2) with the formula derived by Hellmann through generalizing the statistical model of the atom by means of grouping electrons according to orbital momentum.<sup>3</sup> Using Eq. (4), the formula of Hellmann for  $\rho_l(r)$  has the form

$$\rho_l(r) = \frac{2l+1}{2\pi^2 r^2} \left[ (3\pi^2 \rho(r))^{2/3} - \frac{l(l+1)}{r^2} \right]^{1/2}. \tag{5}$$

In so far as imaginary values of  $\rho_l(r)$  have no physical significance, for  $l \neq 0$ ,  $\rho_l(r)$  is non-zero in some interval  $r_1 < r < r_2$ , where  $r_1$  and  $r_2$  are roots of the quantity under the square root in Eq. (5). For the case of  $l = 0$ , we have

$$\rho_0(r) = (3\pi^2 \rho(r))^{1/3} / 2\pi^2 r^2 = K_\mu / 2\pi^2 r^2, \tag{6}$$

where for  $r \rightarrow 0$  we have  $\rho_0(r) \sim r^{-5/2}$  in the atomic case and  $\rho_0(r) \sim r^{-2}$  in the nuclear case. In our case, for  $l = 0$  the integration in Eq. (2) can be performed, and we have

$$\rho_0(r) = (2K_\mu r - \sin(2K_\mu r)) / 4\pi^2 r^3. \tag{7}$$

Thus, for  $r \rightarrow 0$  we have  $\rho_0(r) \rightarrow K_\mu^3 / 3\pi^2$ , and comparison with Eqs. (3) and (4) shows that only protons with  $l = 0$  can be at the origin, as should be the case. For large  $r$ , Eqs. (6) and (7) practically coincide. From analysis of Eq. (2) for  $l \neq 0$ , it follows that  $\rho_l(r) \rightarrow 0$  for  $r \rightarrow 0$  and

has finite real values for arbitrary  $0 < r < \infty$  [in contradistinction to Eq. (5)]. This is in agreement with the behavior of  $\rho_l(r)$  expected from quantum mechanical considerations.

**2. DISTRIBUTION OF PROTON DENSITY WITH ANGULAR MOMENTUM AND SPATIAL DISTRIBUTION OF SHELLS IN THE NUCLEUS**

We now apply Eq. (2) to calculate  $\rho_l(r)$  for protons in a spherically symmetrical nucleus with  $\rho(r)$  in the form of a Fermi distribution,

$$\rho(r) = \rho_0 \left[ 1 + \exp\left(\frac{r-c}{b}\right) \right]^{-1}, \quad (8)$$

where the coefficients  $c$  and  $b$  are determined from the experiments of Hofstadter et al.,<sup>2</sup>

$$c = (1.07 \pm 0.02) A^{1/3} \cdot 10^{-13} \text{ cm},$$

$$b = (0.5455 \pm 0.0682) \cdot 10^{-13} \text{ cm}, \quad (9)$$

and  $\rho_0$  is found by normalizing the total charge to  $Z$  protons in the nucleus.

From Eq. (2) we obtain for the number of protons  $Z_l$  in states with a given  $l$

$$Z_l = 4\pi \int_0^{\infty} r^2 \rho_l(r) dr. \quad (10)$$

Comparison of numerical values obtained by integrating Eqs. (2) and (10) with empirical values is shown in Table I for the particular case of  $\text{Au}_{79}^{197}$ . Instead of the parameters in Eq. (9) we here employ the actual experimental values of Hofstadter's parameters  $\rho_0 = 0.68 \times 10^{38} \text{ cm}^{-3}$ ,  $c = 6.38 \times 10^{-13} \text{ cm}$ ,  $b = 0.528 \times 10^{-13} \text{ cm}$ . The corresponding density distributions  $\rho_l(r)$  are shown in Fig. 1.

From Table I it can be seen that the values of  $Z_l$  agree, in general, with the corresponding values from the shell model, making it possible to assess the correctness of the given  $\rho_l(r)$ . In the final column, the numbers of protons of given  $l$  present in the surface of the nucleus ( $0.9 \rho_0 \leq \rho(r)$

**TABLE I.** Number of protons  $Z_l$  with given  $l$  for  $\text{Au}_{79}^{197}$

Angular momentum $l$	$Z_l$	Nearest integer	According to scheme of Mayer	Number of particles of given $l$ in the surface layer
0	5.65	6	6	1.55
1	12.48	12	12	4.66
2	16.97	17	20	7.61
3	17.93	18	14	9.91
4	15.6	16	18	9.63
5	9.01	9	9	6.03
6	1.27	1	0	0.49

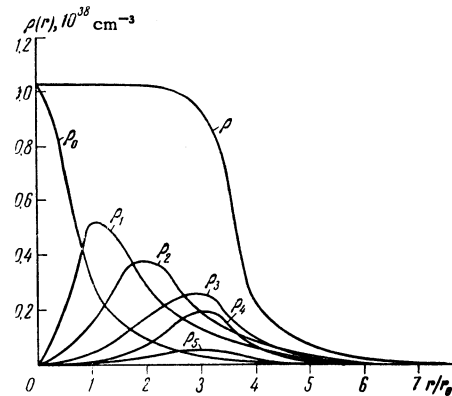


FIG. 1. Distribution of proton density  $\rho_l(r)$  with angular momentum  $l$  for  $\text{Au}_{79}^{197}$ .

$\leq 0.1 \rho_0$ ) are given. From Fig. 1 it can be seen that the behavior found for  $\rho_l(r)$  corresponds to that expected from quantum mechanical calculations. Analogous results have been obtained for other nuclei.

We now analyze how the distribution of radial proton density  $\rho_l(r) r^2$  in states of given  $l$  changes with changing number of protons  $Z$  in the nucleus. The relevant curves for  $l = 0$  and  $l = 1$  are given in Figs. 2 and 3. Let us consider, for example, Fig. 3. Analysis of the change in density from  $\text{Li}_3^6$  ( $Z_1 = 1.05$ ) to  $\text{S}_{16}^{32}$  ( $Z_1 = 6.12$ ) shows that the maximum density gradually increases, the maximum remaining at the same distance from the center, and the quantity  $\rho_l(r) r^2 / Z_l$  for arbitrary  $r$  does not depend upon

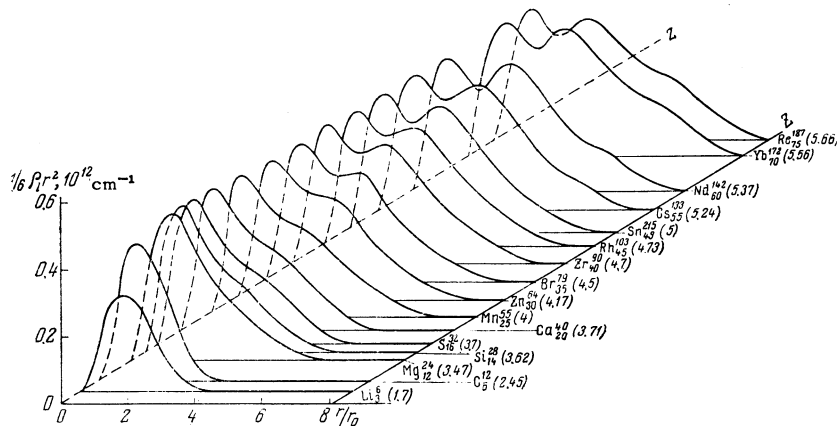


FIG. 2. Dependence of proton radial density  $\rho_l(r) r^2$  on  $Z$  for  $l = 0$ . For light nuclei (up to  $\text{Ca}_{20}^{40}$ ) the experimental parameters  $c$  and  $b$  were employed in Eq. (8) for  $\rho(r)$ . For heavy nuclei,  $c$  and  $b$  were obtained from Eq. (9). The numbers in parentheses after the nucleus give the number of protons found in the data with given  $l$  in the indicated nucleus.

FIG. 3. Dependence of the proton radial density  $\rho_l(r)r^2$  on  $Z$  for the case of  $l = 1$ .

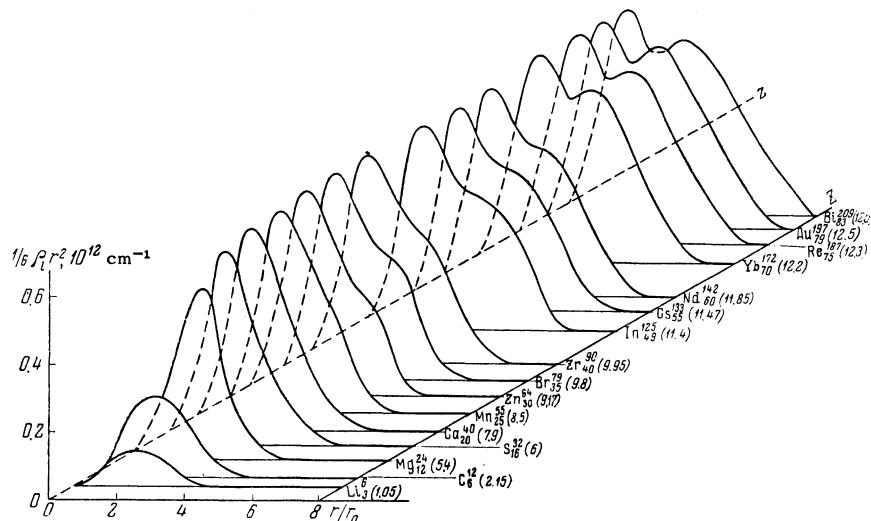


TABLE II. Comparison of the number of protons  $Z_l$  in filled subshells with the Goeppert-Mayer scheme

$l$	$Z_l$ in this work		$Z_l$ according to Mayer	
	first subshell	second subshell	first subshell	second subshell
0	$\approx 2$	$\approx 2$	2	2
1	$\approx 6$	$\approx 6$	6	6

$Z$ . After  $S_{16}^{32}$  the maximum stops growing with increasing  $Z$ , the left part of  $\rho_l(r)r^2$  stops changing, and a deformation in the right part of the curve sets in. Such a behavior of the radial density indicates that the first subshell is filled in the region  $Z = 15$  ( $Z_1 \approx 6$ ). The deformation of the right part continues growing until near  $Nd_{60}^{142}$  ( $Z_1 \approx 12$ ) a second maximum arises; i.e., a second subshell is apparently full. An analogous behavior of the curve continues further. The total numbers of protons in filled subshells, as follow from Figs. 2 and 3, and their comparison with the Goeppert-Mayer scheme are shown in Table II.

Thus, the semi-statistical way of considering the nucleus employed by us makes it possible not only to obtain information about the shell structure

in the nucleus, but also to show the spatial distribution of the shells in the region of their principal maxima (by calculating the distribution curves for the preceding subshells). In particular, these distributions show that both the form and area of a completely filled subshell remain practically unchanged with the growth of further nucleon shells. Analyses of other distributions of total charge (for example, references 4 and 5) also show that shell structure arises; however, less satisfactory agreement with the Goeppert-Mayer scheme is obtained.

<sup>1</sup> S. Golden, Phys. Rev. **110**, 1349 (1958).

<sup>2</sup> R. Hofstadter, Revs. Modern Phys. **28**, 214 (1956).

<sup>3</sup> H. Hellmann, Acta Phys. Chem. URSS **4**, 225 (1936).

<sup>4</sup> L. P. Rapoport and V. A. Filimonov, JETP **27**, 243 (1954).

<sup>5</sup> F. Kligman, JETP **35**, 367 (1958), Soviet Phys. JETP **8**, 255 (1959).